

Design Review II: The Hexapedal Robot

Professor Stolfi
Spring 2018

The Permanents

Mark Cartolano

Sarah Wang

Erika Soto

Alicia Dagle

Kevin Dean

Columbia University
Department of Mechanical Engineering
April 17, 2018

Contents

1	Executive Summary	5
2	Introduction	5
3	Concept Generation and Selection	6
3.1	Legs	6
3.2	Connectivity	7
3.3	Body Design	7
4	Literature Search Results	8
4.1	Internet Search	8
4.2	Journal Search	9
4.3	Patent Search	9
5	Specifications & Parameter Analysis	10
5.1	Leg Modeling Assumptions	10
5.2	Kinematics	11
5.3	Leg Modeling	12
5.4	Dynamics	17
6	Final Design	19
6.1	Leg Dimensions	19
6.2	Leg Stress Analysis	20
6.3	Robot Dimensions	21
6.4	Motor Selection & Mounting	22
6.5	Electronics	23
7	Plan & Problem Analysis (Risks)	24

8	Conclusion	26
9	Reference List	26
10	Acknowledgements	27

List of Figures

1	The forces on the body caused by each leg in the x, y and z component are shown above.	13
2	The ground force F_{Gi} is shown anti parallel to the actuation force F_{Ai} where $\ F_{Gi} \ = \ F_{Ai} \ $. The spring force F_{Si} acts perpendicular to these forces along the direction of the approximated spring model from the point of contact with the ground to the attachment point to the body.	13
3	Leg force locations as defined by α , β , and γ relative to the center of mass of the body [10].	15
4	The top two graphs plot force from legs 135 and 236 respectively against actuation angle ϕ for a complete 360 degree rotation of the legs. The bottom two graphs plot torque from legs 135 and 236 respectively against actuation angle ϕ for a complete 360 degree rotation of the legs.	16
5	Leg geometric characterization and chosen dimensions.	20
6	Stress and displacement results of leg design when a 10lbf is applied.	21
7	Top view of CAD model with associated total dimensions.	21
8	Side view of the top shell of the robot	22
9	Left: Figure of the motor mount assembly. Right: Internal frame	23

1 Executive Summary

The below report has been composed to detail the design and future production of a computer controlled hexapedal robot or RHex for the senior design exhibition in May 2018. The RHex will be an all terrain, WiFi controlled robot featuring a live stream camera feed. The RHex control interface will utilize a server generated by the WiFi module inside the robot. The server is reachable by the user's computer that will display the camera feed and will be controlled by the directional keys on the computer's keyboard. The robot will be able to climb over rubble, brush, and other rough terrain aiding in disaster relief as well as easing search and rescue missions.

2 Introduction

Natural disasters are not a common occurrence but when they do occur, they are detrimental and can result in casualties, deaths, and missing persons. Many different robot designs have been developed to address problems associated with finding missing persons. Debris resulting from landslides, avalanches and earthquakes among other disasters can trap people for weeks on end. The design goal is to manufacture a robot that can tackle any environment to search and find people who have become trapped. The locomotion of the design is based on the movement of a cockroach. The 6-leg, cockroach style gait, mixed with voltage sensors should allow the robot to transition effortlessly from rocky terrain to smooth, flat terrain. To ensure completion of our goal, the robot will first be designed to be operated by a wireless controller. Next, a camera will be attached to allow for visual transmission back to the user. After medium to long distance, wireless control by computer with video feedback has been established, the team will assess the the possibility for the RHex to carry small payloads such as small amounts of food and water as well as adaption to inverted operation.

3 Concept Generation and Selection

The design intent of the team is to create an all terrain RHex, a robot whose motion is modeled after a hexapod and can cross multiple different terrains. The design calls for 6, C-shaped legs with one actuator per leg, all controlled by an on-board Arduino. The gait of the RHex will be established such that 3 legs will be in the same position while the other 3 are in another position, presumably offset by 180 degrees when on flat ground. The RHex will be equipped with a front-facing camera, giving the user access to the field of vision in front of the robot. The camera feed will be broad-casted back to a computer via WiFi where the user will be able to control the motion of the RHex with the computers keyboard.

3.1 Legs

The design chosen is unique and utilizes a C-shaped leg where other designs of all terrain vehicles may use treads, larger wheels, or more humanoid type, jointed legs. Examples of different patents include Patent US 7249640 B2 and Patent US 8789630 B2. The former patent discusses the use of WHEGS, a hybrid of wheels and legs to allow for climbing and running at sustained speeds over 10 body lengths per second. The later of the 2 patents outlines the design of a variable stiffness compliant leg based on the length of the leg. The length can then be altered based on the terrain the RHex is traversing. The patents offered deep insight into the different leg options and materials being used by other individuals. Patent US 6481513 B2 provided the motion which would be modeled by the RHex outlined in this report. The model uses 6 different actuators, 1 per leg, to govern the alternating tripod gait of the robot.

The C-shape leg design, inspired by Boston Dynamics, allows the team to model the shape after a single spring system while allowing for more complex movement options such as jumping obstacles. The spring system acts like a spring in the vertical and horizontal direction, thus when the leg rotates and is compressed, the robot will be propelled forward when the spring expands. The forward movement of the robot is controlled by a 6 leg tripod gait, where the front and rear legs on one side of the robot rotate in unison with the middle

leg on the other side. The remaining 3 legs will rotate in unison as well but will be in a different position than the first set of legs. The RHex will have forward and backward movement in addition to turning capabilities. To turn the robot, one set of legs will engage in the forward direction while the opposite set of legs will engage in the backwards direction, causing the robot to turn in place.

3.2 Connectivity

A front facing camera will be able to provide a live stream feedback to the user. The camera will allow users to assess what is in front of the robot whether that be rough terrain or a person who has been trapped under the rubble of a fallen building. The camera specifically chosen for the prototype is a Sony HDR-AS15 action camera which has been available to the group by one of the members. The camera was chosen within a limited budget and with the capability to offer WiFi video feed. WiFi capabilities allow the user to extend camera ranges offered by Bluetooth without having to equip bulky antennas to the RHex or the computer for radio transmission. Along with transmitting the video feed with WiFi, the direction of the robot will be controlled by WiFi for the same reasons. WiFi allows us to maximize the distance the robot can travel from the user while minimizing real estate on the robot platform and the budget. An Adafruit Hazzah Esp8266 was chosen to sync with the Arduino Mega that will act as the main controller for the RHex. The Hazzah offers WiFi capabilities as well as limited programmability at a cheap price. The Hazzah creates a WiFi signal that is linked to a server, which will receive commands from a website, then in turn communicates those signals to the Mega via transmit and receive pins on the board. The video feed will also be connected to the same website where an optimized user experience will be provided.

3.3 Body Design

The body of the RHex body, composed of aluminum and carbon fiber, will come to a peak on each side. With the intent of the robot being able to face all terrains and disaster relief, the body should be able to face smaller amounts of falling rubble and other debris while remaining light enough to maintain a reasonable speed. Falling debris can puncture

the body or cause damage leading to destruction of the device. Adding a peak to each side, similar to sloped armor on a tank, will strengthen the body, adding survivability to the RHex. In addition, reinforcing the body, the sloped body will keep rubble from settling on top of the robot which could add more stress to the legs.

Aluminum was chosen for the frame to keep the weight of the robot down while maintaining some strength. Steel is too heavy for the purpose of the robot and will limit the material chosen for the legs. Aluminum is a more pliable material that can be manipulated to form the body shape. Although relatively light compared to steel, aluminum would result in too heavy a design if used for the entire body. Instead of aluminum, the group plans to use carbon fiber as a supplement for several parts of the exterior of the body.

4 Literature Search Results

Our literature search focused on optimizing our design by gaining a better understanding of design parameters used by previous RHex robots or similar mechanisms. Our search was divided into three main parts: internet search, journal search, and patent search.

4.1 Internet Search

During our initial internet search, we found that the RHex was originally funded by a 1998 DARPA project that lasted five years. Several prototypes were built with different goals in mind such as walking, jumping, and running. Most of these simple behaviors were achieved using open loop controls while more advanced functions such as line following and bipedal walking required feedback from sensors and on-board cameras [1]. Boston Dynamics designed their own rugged RHex robot which incorporated inverted operation, carried up to 2 kg of payload and featured a teleoperation camera [2]. The University of Pennsylvania's Kod Lab created several variations of the RHex, incorporating modular payload systems and pushing the limit of agility for outdoor rough terrain usage [3].

In each different design, the overall form of the robot was mostly standard; each robot had six legs controlled by six independent actuators which were controlled by an on-board computer. The leg designs varied between robots, and therefore prompted a more thorough

search for the journal and patent sections.

4.2 Journal Search

Most of the journal research was done to examine the legs of the RHex robot, which are critical to the locomotion of this machine. Compliant legs were used on the latest variations of the RHex robots. These are legs that use the stored elastic potential energy from compression to help the robot spring forward with each step. The journal entry, Reliable Stair Climbing in the simple hexapod RHex, provides an in depth comparison of three leg designs. The compass, four bar, and half circle leg each provide unique capabilities to the hexapedal robot, but ultimately the journal concludes that the half circle leg increases stability by increasing the amount of contact points between the leg and terrain [4].

Another journal article discusses how to identify various terrain based on the torque that each leg experiences. The torque is measured using statistical analysis of the current going to each independent motor. A threshold value for current must be provided to serve as a comparison to other potential terrains [5].

The journal article, Modeling of a Hexapod Robot; Kinematic Equivalence to a Unicycle, was used as our primary source to conduct a dynamic analysis. The journal article simplifies each leg to a spring, and allows for the calculation of forces and torque to be executed using MATLAB [6].

4.3 Patent Search

We started our search with Martin Buehler's patent for a hexapedal robot. Buehler is a leader in dynamic locomotion robotic technology and is one of the primary inventors of the hexapedal (RHex) robot. His patent describes the use of six separate actuators that individually control each leg to achieve a tripod gate. We then used this patent to do a category search on relevant designs including compliant leg, hexapedal robot and multipedes [7].

Patent US 7249640 B2 describes a mobile robot capable of running and jumping on rough terrains. Its unique use of WHEGS, a hybrid of wheels and legs, allows for climbing and running at sustained speeds over 10 body lengths per second. This robot also uses an

alternating gait similar to the one employed in our design [8].

Patent US 8789630 B2 outlines the design of a variable stiffness compliant leg for a hexapedal robot. The legs change length to adjust the elasticity and allows the vehicle to adapt to different terrains. Based on the patent, we found that most compliant legs are made out of a composite with high tensile strength such as Delrin or Fiberglass [9].

5 Specifications & Parameter Analysis

5.1 Leg Modeling Assumptions

For simplicity, assumptions were made to model the legs and perform dynamic calculations. Each leg has a circular curvature, which bends under loaded compression. Similar to the RHEX robots, each leg is approximated to behave as a massless linear spring because it is significantly lighter than the robot body [6].

The spring constants for the legs are a function of the material properties and curvature. The uncompressed spring length, l_{0i} , is the diameter of the leg. The spring parameters are then determined using SolidWorks material analysis. The change in length, Δl is also calculated using SolidWorks and observed for a given load. This is representative of approximately $\frac{1}{3}$ the weight of the body. The adjusted spring length l_i and spring constant k can then be determined using the linear spring model (Equations 1- 2);

$$F = -k(l_i - l_{0i}) \quad (1)$$

where

$$\Delta l = l_i - l_{0i} \quad (2)$$

For simplicity, the compression length of the linear spring is assumed not to be time dependent. This oversimplification means that the spring is modeled to be the same compressed length whenever it is in contact with the ground. In this way, the spring is either compressed or uncompressed in a binary manner with no intermediate steps.

5.2 Kinematics

The position and orientation vectors of the center of mass of the robot relative to a global frame are given by equation 3. Here, $x \ y \ z$ are the positions in 3D space and $p \ \pi \ \gamma$ are the Euler angles used to describe orientation. Similarly, the velocity and angular velocity are given by equation 4. Here, $u \ v \ w$ are the velocities in $x \ y \ z$ coordinate space relative to the body system. Similarly, $p \ q \ r$ are the angular velocities in spherical coordinates.

$$\mathbf{n} = [x \ y \ z \ \rho \ \pi \ \gamma]^T \quad (3)$$

$$\mathbf{v} = [u \ v \ w \ p \ q \ r]^T \quad (4)$$

Linear and angular velocity transformation matrices can then be applied to transform the coordinates from the ground frame G to the body frame B as indicated by equations 5- 6 where $\mathbf{R}_B^G(\boldsymbol{\Theta})$ is the rotation matrix and $\mathbf{T}(\boldsymbol{\Theta})$ is the transformation matrix.

$$\mathbf{R}_B^G(\boldsymbol{\Theta}) = \begin{pmatrix} \cos \gamma \cos \pi & -\sin \gamma \cos \rho + \cos \gamma \sin \pi \sin \rho & \sin \gamma \sin \rho + \cos \gamma \cos \rho \sin \pi \\ \sin \gamma \cos \pi & \cos \gamma \cos \rho + \sin \gamma \sin \pi \sin \rho & -\cos \gamma \sin \rho + \sin \gamma \cos \rho \sin \pi \\ -\sin \pi & \cos \pi \sin \rho & \cos \pi \cos \rho \end{pmatrix} \quad (5)$$

$$\mathbf{T}(\boldsymbol{\Theta}) = \begin{pmatrix} 1 & \sin \rho \tan \pi & \cos \rho \tan \pi \\ 0 & \cos \rho & -\sin \rho \\ 0 & \sin \rho / \cos \pi & \cos \rho / \cos \pi \end{pmatrix} \quad (6)$$

where:

$$\boldsymbol{\Theta} = [\rho \ \pi \ \gamma]^T \quad (7)$$

These are integrated into the matrix $J(\boldsymbol{\Theta})$ (equation 8) and can be used to write the velocity matrix $\dot{\mathbf{n}}$ in the body frame B in terms of ν , the velocity matrix in the ground frame G as demonstrated in equation 9.

$$\mathbf{J}(\boldsymbol{\Theta}) = \begin{pmatrix} \mathbf{R}_B^G(\boldsymbol{\Theta}) & \mathbf{0}_{3 \times 3} \\ \mathbf{0}_{3 \times 3} & \mathbf{T}(\boldsymbol{\Theta}) \end{pmatrix} \quad (8)$$

$$\dot{\mathbf{n}} = \mathbf{J}(\boldsymbol{\Theta})\mathbf{v} \quad (9)$$

5.3 Leg Modeling

The spring force and ground force on each leg is first calculated using the equations 10- 11:

$$F_{Si} = -k_i(l_i - l_{0i}) \quad (10)$$

$$F_{Gi} = \frac{\tau_{\phi i}}{l_i} \quad (11)$$

The force on the body from each leg i can then be represented as follows in equation 12 where the x y z components of force are shown in figure 1. The ground force, F_{Gi} , and spring force, F_{Si} , are then depicted in figure 2.

$$\mathbf{F}_i^b = \begin{bmatrix} F_{xi} \\ F_{yi} \\ F_{zi} \end{bmatrix} = \begin{bmatrix} -\sin \phi_i & -\cos \phi_i \\ 0 & 0 \\ -\cos \phi_i & \sin \phi_i \end{bmatrix} \begin{bmatrix} F_{Si} \\ F_{Gi} \end{bmatrix} \quad (12)$$

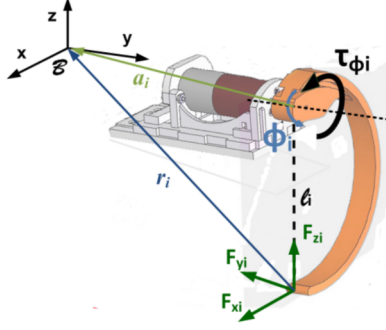


Figure 1: The forces on the body caused by each leg in the x, y and z component are shown above.

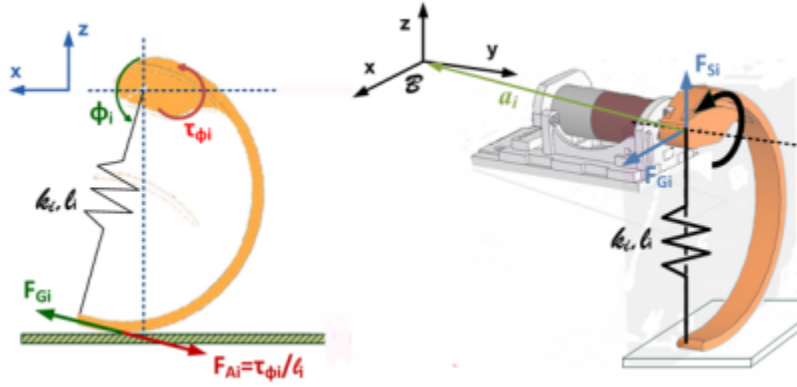


Figure 2: The ground force F_{Gi} is shown anti parallel to the actuation force F_{Ai} where $\| F_{Gi} \| = \| F_{Ai} \|$. The spring force F_{Si} acts perpendicular to these forces along the direction of the approximated spring model from the point of contact with the ground to the attachment point to the body.

The sum of these forces for each leg then represents the force vector F^B applied to the body in the B frame as demonstrated in equation 13 and the actuation moments with respect to the center of gravity of the body is then shown by equation 14.

$$\mathbf{F}^B = \begin{bmatrix} F_x \\ F_y \\ F_z \end{bmatrix}^B = \sum_{i=1}^6 leg_i \mathbf{F}_i^B \quad (13)$$

$$\boldsymbol{\tau}^B = \begin{bmatrix} \tau_x \\ \tau_y \\ \tau_z \end{bmatrix}^B = \sum_{i=1}^6 leg_i \boldsymbol{\tau}_i^B \quad (14)$$

where

$$leg_i = \begin{cases} 1 & \text{leg } i \text{ is in stance} \\ 0 & \text{leg } i \text{ is in flight} \end{cases} \quad (15)$$

In general, the actuation moment or torque, τ^B is calculated by the cross product of force and the distance between its application point and the center of mass. This is expressed by equation 16 but can cleverly be rewritten using the property that the cross product is equivalent to the multiplication of a skew symmetric matrix as shown in equation 17 where the subscripts of a indicate the matrix indices of the vector.

$$\boldsymbol{\tau}^B = \mathbf{a}_i \times \mathbf{F}_i^B \quad (16)$$

$$\boldsymbol{\tau}^B = \mathbf{a}_i \times \mathbf{F}_i^B = \mathbf{S}(\mathbf{a}_i) \mathbf{F} = \begin{bmatrix} 0 & -a_3 & a_2 \\ a_3 & 0 & -a_1 \\ -a_2 & a_1 & 0 \end{bmatrix} \mathbf{F} \quad (17)$$

where the location matrices a_i for each leg are given by equations 18 where $\alpha, \beta, \text{ and } \gamma$ are used to define the distance of each leg from the center of mass of the body as depicted by figure 3.

$$\begin{aligned} \mathbf{a}_1 &= [\alpha \quad \beta \quad 0]^T & \mathbf{a}_2 &= [\alpha \quad -\beta \quad 0]^T & \mathbf{a}_3 &= [0 \quad \gamma \quad 0]^T \\ \mathbf{a}_4 &= [0 \quad -\gamma \quad 0]^T & \mathbf{a}_5 &= [-\alpha \quad \beta \quad 0]^T & \mathbf{a}_6 &= [-\alpha \quad -\beta \quad 0]^T \end{aligned} \quad (18)$$

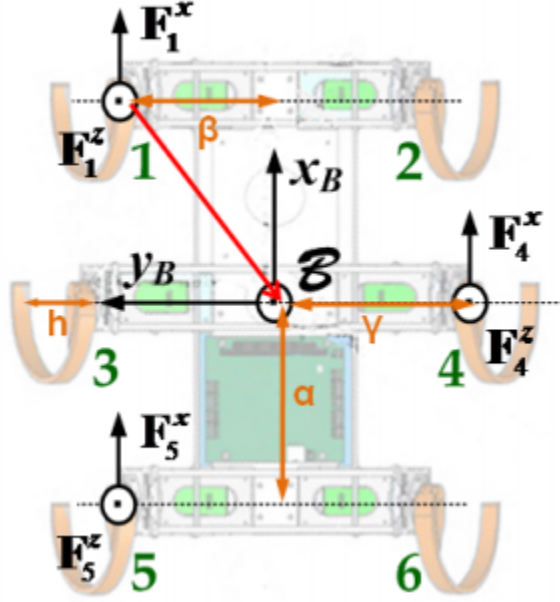


Figure 3: Leg force locations as defined by α , β , and γ relative to the center of mass of the body [10].

The torque on the body relative to the body frame can then be calculated for each leg as follows in equation 19. Finally, the force and torque on the body from each set of tripod legs (145 and 236 respectively) can be described relative to the body frame of the robot as τ_A in equation 20 [6].

$$\begin{aligned}
 \tau_1^B &= \begin{bmatrix} 0 & 0 & \beta \\ 0 & 0 & -\alpha \\ -\beta & \alpha & 0 \end{bmatrix} \begin{bmatrix} F_{x1} \\ 0 \\ F_{z1} \end{bmatrix} & \tau_2^B &= \begin{bmatrix} 0 & 0 & -\beta \\ 0 & 0 & -\alpha \\ \beta & \alpha & 0 \end{bmatrix} \begin{bmatrix} F_{x2} \\ 0 \\ F_{z2} \end{bmatrix} & \tau_3^B &= \begin{bmatrix} 0 & 0 & \gamma \\ 0 & 0 & 0 \\ -\gamma & 0 & 0 \end{bmatrix} \begin{bmatrix} F_{x3} \\ 0 \\ F_{z3} \end{bmatrix} \\
 \tau_4^B &= \begin{bmatrix} 0 & 0 & -\gamma \\ 0 & 0 & 0 \\ \gamma & 0 & 0 \end{bmatrix} \begin{bmatrix} F_{x4} \\ 0 \\ F_{z4} \end{bmatrix} & \tau_5^B &= \begin{bmatrix} 0 & 0 & \beta \\ 0 & 0 & \alpha \\ -\beta & -\alpha & 0 \end{bmatrix} \begin{bmatrix} F_{x5} \\ 0 \\ F_{z5} \end{bmatrix} & \tau_6^B &= \begin{bmatrix} 0 & 0 & -\beta \\ 0 & 0 & \alpha \\ \beta & -\alpha & 0 \end{bmatrix} \begin{bmatrix} F_{x6} \\ 0 \\ F_{z6} \end{bmatrix}
 \end{aligned} \tag{19}$$

$$\tau_A = \begin{bmatrix} F^B \\ \tau^B \end{bmatrix} = \begin{cases} \begin{bmatrix} F_1^B + F_4^B + F_5^B \\ \tau_1^B + \tau_4^B + \tau_5^B \end{bmatrix}, & \text{legs 1-4-5 on the ground} \\ \begin{bmatrix} F_2^B + F_3^B + F_6^B \\ \tau_2^B + \tau_3^B + \tau_6^B \end{bmatrix}, & \text{legs 2-3-6 on the ground} \end{cases} \quad (20)$$

These body forces and torques for each set of legs can then be plotted against the actuation angle, representative of the leg rotations. This has been done for an angle from 0 to 360 degrees showing approximately one rotation in the gait of the robot in figure 4.

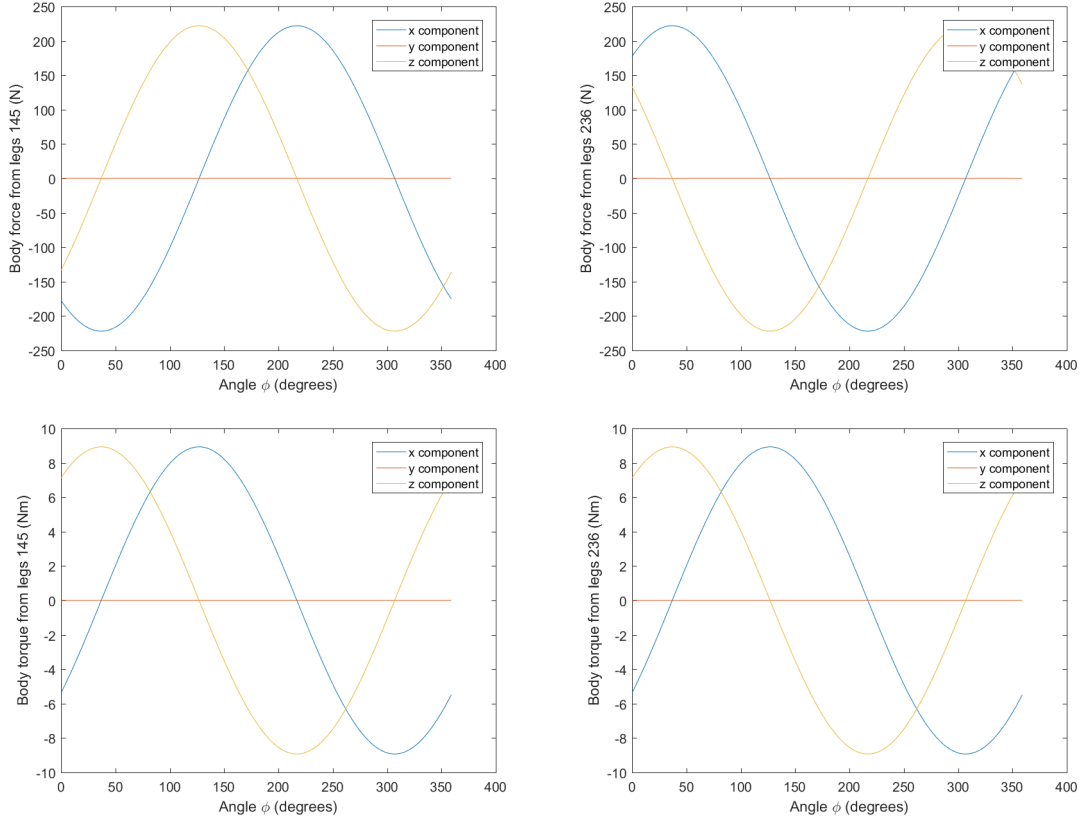


Figure 4: The top two graphs plot force from legs 135 and 236 respectively against actuation angle ϕ for a complete 360 degree rotation of the legs. The bottom two graphs plot torque from legs 135 and 236 respectively against actuation angle ϕ for a complete 360 degree rotation of the legs.

Here, it is observed that the y component of force is zero as expected while the x and z components are out of phase between the two sets of legs 135 and 246. For torque, it can be

observed that the x, y and z components are the same for both sets of legs.

5.4 Dynamics

To define the dynamics for this system, the inertia matrix of the rigid body is first defined as follows in equation 21:

$$\mathbf{M}_{RB} = \begin{bmatrix} m\mathbf{I}_{3 \times 3} & \mathbf{0}_{3 \times 3} \\ \mathbf{0}_{3 \times 3} & \mathbf{I}_0 \end{bmatrix} \quad (21)$$

where $\mathbf{I}_{3 \times 3}$ is a 3 by 3 identity matrix and \mathbf{I}_0 is an inertia matrix of diagonals with I_x , I_y and I_z components. The Coriolis matrix $\mathbf{C}_{RB}(\boldsymbol{\nu})$ can then be written in terms of the skew symmetric matrix of linear and angular velocity components $\boldsymbol{\nu}_1$ and $\boldsymbol{\nu}_2$ as follows in equation 22:

$$\mathbf{C}_{RB}(\boldsymbol{\nu}) = \begin{bmatrix} \mathbf{0}_{3 \times 3} & -m\mathbf{S}(\boldsymbol{\nu}_1) \\ -m\mathbf{S}(\boldsymbol{\nu}_1) & -\mathbf{S}(\mathbf{I}_0\boldsymbol{\nu}_2) \end{bmatrix} \quad (22)$$

where $\boldsymbol{\nu} = \begin{bmatrix} \boldsymbol{\nu}_1 & \boldsymbol{\nu}_2 \end{bmatrix}^T$ and therefore $\boldsymbol{\nu}_1 = \begin{bmatrix} u & v & w \end{bmatrix}^T$ and $\boldsymbol{\nu}_2 = \begin{bmatrix} p & q & r \end{bmatrix}^T$ from equation 4. The vector of generalized external forces, $\boldsymbol{\tau}_{RB}$, can then be derived as follows in equation 23:

$$\boldsymbol{\tau}_{RB} = \mathbf{M}_{RB}\dot{\boldsymbol{\nu}} + \mathbf{C}_{RB}(\boldsymbol{\nu})\boldsymbol{\nu} \quad (23)$$

The vector of generalized forces and moments can again be rewritten as equation 24 as follows:

$$\boldsymbol{\tau}_{RB} = \boldsymbol{\tau}_A - g(\boldsymbol{\eta}) \quad (24)$$

where $\boldsymbol{\tau}_A = \begin{bmatrix} \mathbf{F}^B \\ \boldsymbol{\tau}^B \end{bmatrix}$ is the vector of actuation forces and $g(\boldsymbol{\eta}) = \begin{bmatrix} \mathbf{f}_g^B \\ \mathbf{r}_{CG} \times \mathbf{f}_g^B \end{bmatrix}$ is the vector of gravitational forces and moments. In this form, $\mathbf{f}_g^B = \mathbf{R}_B^G(\boldsymbol{\Theta})^{-1} \begin{bmatrix} 0 & 0 & -mg \end{bmatrix}^T$. Combining

these equations, one can write the 6 degree of freedom dynamic equations for forces and torques in the x, y, z components as following in equations 25 - 30.

$$F_x = m\dot{u} + mwq - mvr + mgsin\pi \quad (25)$$

$$F_y = m\dot{v} - mwp + mur - mgsinpcos\pi \quad (26)$$

$$F_z = m\dot{w} + mvp - muq - mgcospcos\pi \quad (27)$$

$$\tau_x = I_x\dot{p} + I_zrq - I_yqr \quad (28)$$

$$\tau_y = I_y\dot{q} - I_zrp + I_xpr \quad (29)$$

$$\tau_z = I_z\dot{r} - I_yqp - I_xpq \quad (30)$$

To simplify calculations, it is assumed that the angular velocities p and q will always remain very close to zero because the rotational motion along x and y axis in the body frame is negligible. Similarly, the lateral force F_y in the body frame is assumed to be zero due to the geometry of the robot's walking gait. Considering motion in a horizontal plane for this simple analysis, the roll angle ρ and pitch angle π will also remain close to zero. By setting these variables equal to zero, the following simplifications can be made in equations 31 - 33 where there is now a 3-DOF dynamic system:

$$F_x = m\dot{u} - mvr \quad (31)$$

$$0 = m\dot{v} + mur \quad (32)$$

$$\tau_z = I_z\dot{r} \quad (33)$$

The 3-DOF kinematic equations can then be derived from equation 9 above to result in equation 34 - 36 as follows.

$$\dot{x} = u \cos \phi - \nu \sin \phi = u \cos \phi \quad (34)$$

$$\dot{y} = u \sin \phi + \nu \cos \phi = u \sin \phi \quad (35)$$

$$\dot{\phi} = r \quad (36)$$

These dynamic and kinematic equations are further simplified by accounting for the fact that the actuation forces do not significantly affect the movement in the y-direction and the linear velocity along the y-axis, ν , can therefore be approximated to equal zero. This yields the following in equations 37 - 41 [6].

$$\dot{x} = u \cos \phi \quad (37)$$

$$\dot{y} = u \sin \phi \quad (38)$$

$$\dot{\phi} = r \quad (39)$$

$$F_x = m\dot{u} \quad (40)$$

$$\tau_z = I_z \dot{r} \quad (41)$$

6 Final Design

6.1 Leg Dimensions

The Hexapedal legs are almost semicircle, with a slightly extended arch for the attachment point as well as an extended foot section for extra points of contact. The dimensions of the legs are further illustrated in figure 5, which numerically characterizes the leg sizing and shape. Included in figure 5 is the sizing of the legs chosen and used in simulation testing.

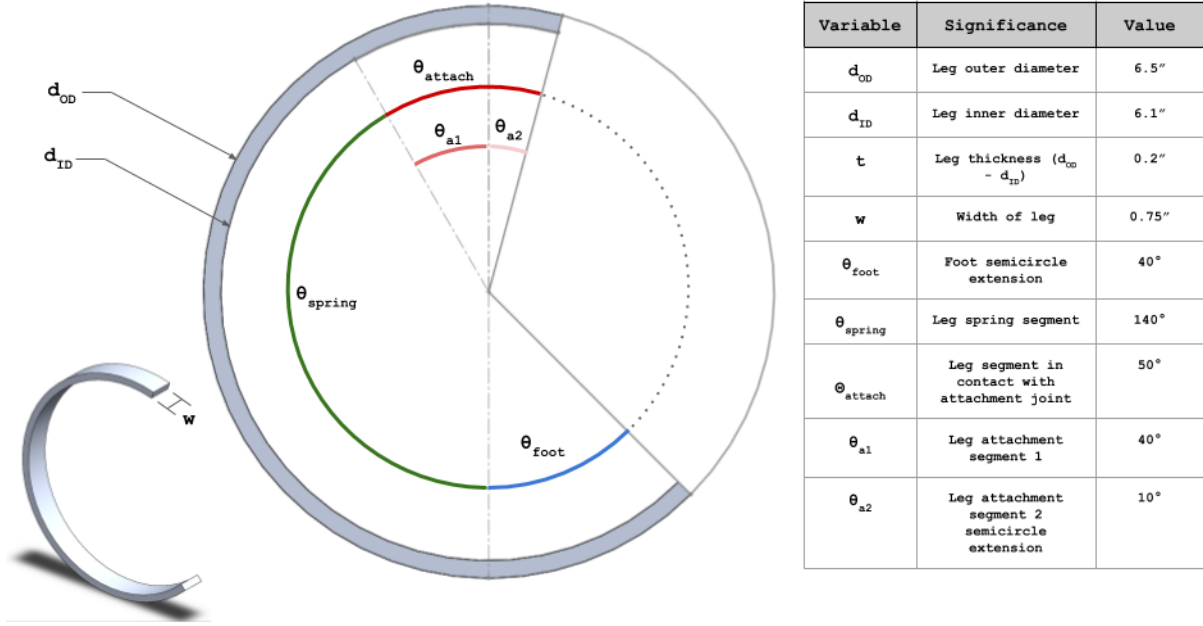


Figure 5: Leg geometric characterization and chosen dimensions.

6.2 Leg Stress Analysis

As required in the kinematic and leg modeling simulations, SolidWorks was used to acquire the linear spring k constant as well as the change in spring length Δl . Using the built in SolidWorks Simulation tool, the stresses and deformation of the leg were computed using a load of 10 lbf, making the assumption that the roughly 30 lb weight of the robot is evenly distributed among the three legs according to the alternating tripod gait.

In this setup, the leg is fixed at the section where it attaches to the leg attachment clamping piece. The load acting on the leg is the ground normal force pushing against the weight on that leg. Figure 6 show the results of the computational analysis performed by SolidWorks.

According to the results, the leg maintained a minimum safety factor of 1.173 at the section with the highest stresses under a 10 lbf load. From the displacement, it was determined that k is 10308.74 N/m and Δl is 4.315 mm. Further investigation of the leg geometry will be carried out to optimize leg strength and elasticity.

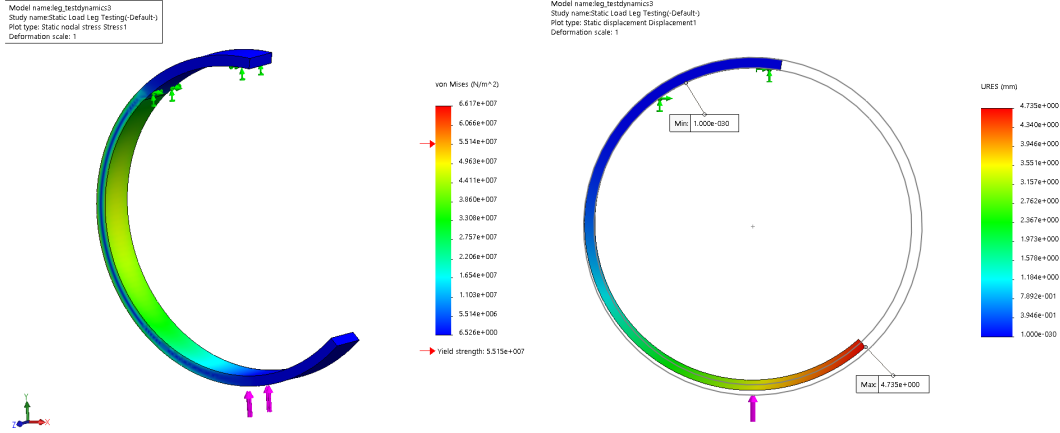


Figure 6: Stress and displacement results of leg design when a 10lbf is applied.

6.3 Robot Dimensions

In order to minimize the length of the robot, the legs must be attached in an offset position because of the six legged design of the robot. This consequently increases the total width of the robot. After a few designs, the optimal size based on our motor and electronic selections is approximately 23 inches in length by 16.5 inches at wheel offset, which can be seen below in 7.

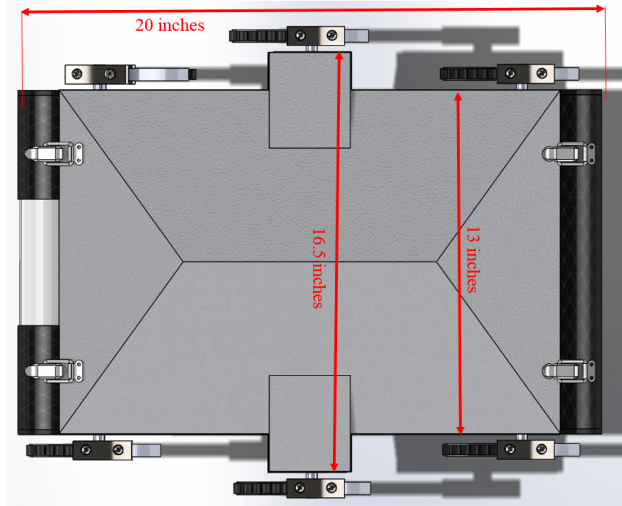


Figure 7: Top view of CAD model with associated total dimensions.

Since this robot is designed to encounter rocky and unstable terrain, the top is designed with a slope so that any potential rubble or debris that it may encounter will not entrap the robot.

A later level of success is inverted operation so the design for the top was kept symmetric, which meant keeping the pitch small so that the robot will not have trouble traversing rocky terrain. The pitch of the roof is 12.5 degrees which can be seen below in figure 8 which leads to a total height of the body to be 6.25 inches from peak to peak.

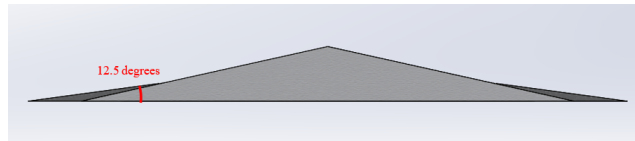


Figure 8: Side view of the top shell of the robot

6.4 Motor Selection & Mounting

Selecting motors for this project was particularly challenging, as they had to be robust enough to support high torque maneuvers (such as obstacle climbing and inclines), provide decent enough shaft speeds for faster gaits, and be relatively cheap due to budgetary constraints as our robot requires six motors. We concluded that DC brushed motors with a built-in planetary reduction gearbox would suit our requirements well.

Based on the literature search and preliminary calculations, the motor torque requirements were set as a continuous operating torque of at least 1.5 N-m and a stall torque of at least 5 N-m. Following suit with previous RHex electronics, we included a factor of safety of around 2 for torque requirements to ensure our motors would be up to the task. As for motor speed requirements, we found that previous RHex robots could maneuver through many terrains with a slow and fast walking speed with a shaft speed of 0.7 Hz - 1.7 Hz respectively. Based on this information, we made the requirement that the motor could handle 1 Hz speeds at least so we could achieve a decent top speed of about 1.75 ft/s. After finding a dozen motors that would meet our requirements and fit our price range, a trade off matrix was created, weighing in encoder quality, weight, price, factor of safety for motor torques, stall torque, and speed. From this analysis, we selected the 84 RPM HD Planetary Gearmotor (with Encoder) with an operating torque of 1.37 N-m and 9.5 N-m stall torque with a no load speed of 84 RPM. This motor was also the most cost effective and has a built

in precise 48 PPR Hall effect magnetic encoder.

Since the motors for each leg will encounter a high level of torque during operation, the motor mount was designed with the intent of minimizing the amount of torque that is directly applied to the motor shaft. The leg shaft is a D-shaft so that it can handle the high RPM and torque and is set between two bearings to minimize the torque. In order to shorten the width of the robot, the motors are set to the side of the leg shaft and are connected via timing belt. This can be seen below in figure 9.

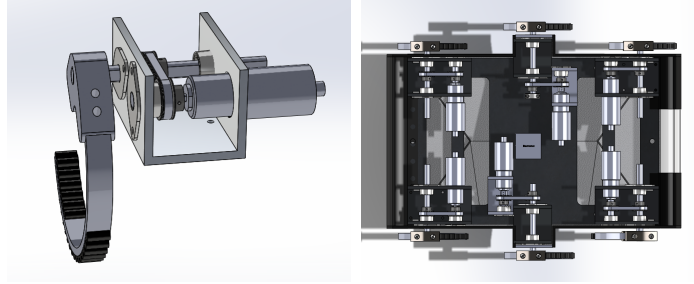


Figure 9: Left: Figure of the motor mount assembly. Right: Internal frame

Each leg is operated independently so each leg includes its own motor mount assembly which is screwed into the aluminum frame structure. The total internal assembly can be seen above in figure 9.

6.5 Electronics

The electronics of the RHex system is unique in that it requires high current draw from the motors, yet each motor must be individually controlled. Each leg has its own dedicated motor, motor controller, and current sensor. The motor controller selected was the 10A Bi-directional DC Motor Driver. This driver operates at the optimal motor voltage (12V) and is able to provide continuous current of up to 10A and peak current of 30A for 10 seconds, significantly higher than the continuous motor current draw of 3.34A and stall current draw of 20A. The built in Hall effect encoders on the motor will work in conjunction with these motor controllers to create a closed feedback loop for precise and synchronized leg control. The current sensor will be used to collect data to measure how hard the motor is working,

giving the robot the ability to identify the difficulty of the current terrain.

Similar to previous RHex electronic design, we will be using two Lithium Polymer batteries to power the leg motors, assigning three motor systems connected parallel to each battery. LiPos were chosen due to their high energy density, smaller sizes, and affordability. Based on the continuous current draw rating of the motors (3.34A), we were able to calculate the run time of our robot depending on the capacity (mAh) of the LiPo. The Turnigy 5000mAh 3S 20C Lipo Pack was chosen, as it will provide the motors with 11.1V and 125A continuous current and 175A burst current, much higher than the power requirements of the three motors (10.02A continuous, 60A peak). The 5000mAh capacity will allow us to run our robot for 30 minutes if we use two batteries. At the end of the LiPo's life, a Low Voltage Cutoff switch or a built in function on the Arduino will turn off the robot so that the LiPo cell voltage doesn't reach dangerously low levels. We also will be getting a 7.4V 1000mAh LiPo battery to independently power the Arduino micro controller to avoid having to use a step down circuit.

In terms of controls, an Arduino MEGA 2560 R3 will be the micro controller for the robot, receiving all of the sensor data and running the gait commands. The Arduino will receive instruction from a human operator, who will connect to the robot using an on-board WiFi module. To get positioning, velocity and acceleration information, our robot will contain an Inertial Measurement Unit (IMU) for Cartesian and angular data recording.

7 Plan & Problem Analysis (Risks)

Moving forward, our plan to complete the RHex by May is comprised of four main sections: finalize dynamics and simulations, fabrication, assembly, and optimization. Within the next two weeks, we plan on finalizing our simulation using Simulink and incorporating our dynamic equations. This will present us with viable expectations with regard to the gait of our robot.

During our fabrication process, we will be creating the six C-shaped legs using fiberglass. This material poses a potential risk due to its lower strength and more difficult manufacturing

process. Despite these risks, fiberglass was chosen based on our conducted motion analysis and references of past RHex robots. The force analysis along with Robert Stark's suggestions, show that fiberglass is a suitable material to support the weight of the body while offering a sufficiently high spring coefficient for the RHex to operate. Other materials such as aluminum and steel were considered but would weigh too much. The legs would weigh about 6 pounds if made from steel, and approximately 1.5 if made from aluminum. Fiberglass, even though not as strong as either of the two metals, results in a weight of approximately 1 pound for all six legs. The weight difference is small, but fiberglass is more elastic than the aluminum, making it more favorable. To counteract the reduced strength of the fiberglass, we will also apply carbon fiber to each leg. Carbon fiber can be expensive and potentially difficult to work with. The cost should be offset by material acquired from the machine shop and formula FSAE shop. With the group lacking prior experience with carbon fiber, we will seek guidance from Robert Stark on the preparation and manufacturing of carbon fiber sheets to be used for the design.

We will also be ordering our motors and electronics within the next two weeks and creating a single motor mount and leg for testing. One of our main concerns is staying under budget, especially when considering the high cost of motors. In order to ensure that we do not damage our motors or electronics during our assembly period and therefore spend more of our budget on reordering, we will be testing one leg and ensuring its successful completion. Once one leg operates properly without damaging any parts, the same setup will be replicated inside the body of the RHex for all the legs. The group also plans to order a few extra of each part in case of malfunctions. Following this process will also ensure we have a foundation for our code and more time to improve it during our testing phase.

During the assembly period, we will assemble all of our components and focus solely on finalizing the physical aspects of our design. Based on our current plan, we expect to have approximately three weeks to optimize our design. This time will be spent on improving our code and addressing any other issues we did not plan for. This is also when we will

incorporate our camera and finalize our WiFi module. A major risk in the performance of the RHex when used in the field would be poor WiFi connectivity. While conducting testing on Columbia's campus should be unaffected, testing the Rhex in a remote location can prove challenging. A WiFi hotspot can be established using a mobile device but hotspots may not provide the user with the desired range for the RHex. To combat this issue, the group would suggest setting up a WiFi hotspot or using cellular data.

8 Conclusion

This report details our plan to manufacture a computer-controlled, all terrain hexapedal robot. The main components of the design include C-shaped compliant legs, control interface utilizing a WiFi module, and camera feed to aid in the control of the robot. Given our budget and time constraints, our group will make use of the best materials and equipment feasible. With a larger budget and adequate time, we suggest that our RHex could be scaled to serve as a search and rescue robot and potentially assist in situations of disaster.

9 Reference List

- [1] Kantor, George. Summary of the RHex Robot Platform. Summary of the RHex Robot Platform
- [2] RHex Devours Rough Terrain RHex — Boston Dynamics, 2018
- [3] Penn Engineering GRASP Lab. RHex. Kodlab
- [4] Moore, E.z., et al. Reliable Stair Climbing in the Simple Hexapod 'RHex'. Proceedings 2002 IEEE International Conference on Robotics and Automation (Cat. No.02CH37292)
- [5] Ordonez, Camilo, et al. Terrain Identification for RHex-Type Robots. Unmanned Systems Technology XV, 2013
- [6] D. Panagou, H. Tanner. "Modeling of a Hexapod Robot; Kinematic Equivalence to a Unicycle," Newark, DE.

- [7] Patent US 6481513 B2
- [8] Patent US 7249640 B2
- [9] Patent US 8789630 B2
- [10] H. Komsuoglu, K. Sohn, R. J. Full, and D. E. Koditschek, A physical model for dynamical arthropod running on level ground, in Proc. of the 11th International Symposium on Experimental Robotics, 2008, Athens, Greece, July 2008.

10 Acknowledgements

It is a pleasure to acknowledge assistance from the laboratory staff in the mechanical engineering laboratories.